Theoretical Study on Low-Lying Electronic States of NiH_2

Wenli Zou and James E. Boggs*

Institute for Theoretical Chemistry, Chemistry and Biochemistry Department, The University of Texas at Austin, Austin, Texas 78712-0165

Received: November 14, 2007; In Final Form: January 28, 2008

The low-lying electronic states of the NiH_2 molecule were investigated by using the MCQDPT2 method. In order to accurately describe the strong correlation derived from the nickel $3d^9$ super-configuration, a set of diffuse secondary 3d′ orbitals were included in the active space, yielding a large active space of 12 electrons in 13 orbitals. It is shown that the absolute minimum energy configuration of NiH_2 is bent, in agreement with the experimental observation. The global ground state is $^1A_1$ (or A_1 in the spin−orbit coupling case), whereas the lowest linear state is $^3\Delta_g$ (or 3_g). Some other cheaper single-configurational and multi-configurational methods were also used to study both states, and their shortcomings are discussed. Our theoretical results suggest that the arrangement of the experimental frequencies of NiH_2 and NiD_2 may be incorrect.

I. Introduction

NiH_2 plays an important role in the widely used nickel−hydrogen batteries. Nevertheless, although NiH_2 is the simplest triatomic nickel(II) molecule, its electronic structure is, in fact, very involved and not fully understood. In the 1920s, Schlenk and Weichselfelder[1,2] reported the existence of NiH_2 for the first time. During the past three decades, there have been some experimental[3] and theoretical[3−14] studies on the NiH_2 molecule. It has been found experimentally that the stable structure of NiH_2 is bent,[3] but the theoretical results are quite different from each other. In the early multireference configuration interaction (MR-CI)[5−7] and semiempirical MINDO[8] computations, as well as the recent complete active space multi-configuration self-consistent field (CASSCF),[3] second-order Møller-Plesset perturbation theory (MP2),[13] and density functional tight-binding (DFTB)[14] computations, a linear ground configuration was obtained, in contrast with the experimental observation. By using density functional theory (DFT) and quadratic configuration interaction with single and double excitations (QCISD), Barron et al.[11] reported a bent ground state $^1A_1$, but the energy difference between the two geometries (and its sign) showed a strong dependence on the basis sets and the methods. Subsequently, Barysz and Papadopoulos[12] obtained the bent ground state again by using complete active-space second-order perturbation theory (CASPT2) with a large active space (12 electrons in 11 orbitals) but they neither described the active orbitals in detail nor explained why this active space was used. In addition, it seems that Filatov et al.[9] also correctly obtained the bent ground state $^1A_1$ using a semiempirical method, but their lowest linear state was not $^3\Delta_g$ as in the other theoretical researches.

Among these previous theoretical studies, it should be noted that the strong correlation derived from nickel 3d orbitals has neither been paid much attention to nor discussed in detail. As an investigation of the strong correlation problem, we have performed three groups of multi-configurational tests.

- State-averaged CASSCF (SA-CASSCF)[15,16] with an active space of 12 electrons in 8 orbitals (i.e., Ni 3d4s + H 1s + H 1s), denoted as (12,8), and subsequent internal-contracted MR-CI with single and double excitations as well as Davidson's correction (ic-MR-CISD+Q),[17] computed using the MOLPRO program package.[18] The resulting numbers of configuration state functions (CSFs) in reference space and external space are on the order of 10^1 and 10^5, respectively.
- Some researchers believe that the nickel 4p orbitals should be included in the active space in order to obtain better excitation energies. This will result in SA-CASSCF with an active space of 12 electrons in 11 orbitals (i.e., Ni 3d4s4p + H 1s + H 1s), denoted as (12,11). In the subsequent ic-MR-CISD+Q calculation, the occupation restriction of $4p^n$ is applied where $n = 0-2$. The resulting numbers of CSFs in reference space and external space are on the order of 10^3 and 10^6, respectively.
- The graphical unitary group approach (GUGA)-based SA-CASSCF[19] with an active space of 12 electrons in 13 orbitals (Ni 3d4s3d′ + H 1s + H 1s; see later explanation about the 3d′ orbitals), denoted as (12,13), and subsequent second-order multi-configurational quasi-degenerate perturbation theory (MC-QDPT2),[20] computed using the PC-GAMESS program package.[21] Compared with the second method, the main difference is that the nickel 4*p* orbitals are replaced by nickel 3d′. The resulting numbers of CSFs in reference space and external space are, respectively, on the order of 10^5 and 10^7.

The tests were made assuming a linear structure, and the bond length of 1.55 Å was used. The basis sets will be described later.

The detailed results are given in the Supporting Information I. Compared with the MCQDPT2(12,13) excitation energies, it is found that the energies of gerade states are fairly good with the mean absolute error (MAE) of only 0.07 eV, but the MAEs of ungerade states of both ic-MR-CISD+Q(12,8) and ic-MR-CISD+Q(12,11) are 0.45 and 0.24 eV, respectively. The reason is that the gerade states come from the Ni $3d^8$ super-configuration, whereas the ungerade states from Ni $3d^9$. It is well-known that 3d orbitals occupied with $n + 1$ electrons are more diffuse than the ones with n electrons,[22,23] resulting in the correlation energy inaccuracy in the ungerade states of linear NiH_2 being

* Corresponding author. Phone: 512-471-7525. Fax: 512-471-8696. E-mail: james.boggs@mail.utexas.edu.

10.1021/jp710881c CCC: $40.75
Published on Web 03/19/2008

TABLE 1: Map Relation of $D_{\infty h}$, D_{2h}, C_{2h}, C_{2v}, and C_s Point Groups[26]

$D_{\infty h}$ ($C_{\infty z}$)	D_{2h} (C_{2z})	C_{2h} (C_{2z})	C_{2v} (C_{2z})	C_s (σ_{hx})
Σ^+_g	A_g	A_g	A_1	A′
Σ^-_g	B_{1g}	A_g	B_2	A′
Π_g, Φ_g	$B_{3g} + B_{2g}$	$2B_g$	$A_2 + B_1$	2A″
Δ_g, Γ_g	$A_g + B_{1g}$	$2A_g$	$A_1 + B_2$	2A′
Σ^+_u	B_{1u}	A_u	B_1	A″
Π_u	$B_{3u} + B_{2u}$	$2B_u$	$A_1 + B_2$	2A′
Δ_u	$A_u + B_{1u}$	$2A_u$	$A_2 + B_1$	2A″

much larger than that in the gerade states. Therefore the distinct occupations and radial extensions of the 3d orbitals in $3d^9$ and $3d^8$ super-configurations require a fine and balanced description of the different electron correlation effects.

The situation in bent NiH_2 is similar, but it is much more complex because the linear symmetry disappears and the gerade and ungerade orbitals as well as the states from the linear configuration mix with each other.

As a remedy for this problem, it has been suggested to simply shift the potential energy surfaces (PESs) by an energy which is estimated from the atomic (or ionic) separation. However, this scheme is questionable for the whole PES because the energy correction changes along with the structure.[24] As for the bent configuration, it is impossible to obtain the empirical energy correction since strong interactions and mixtures exist between the two kinds of super-configuration.

As another method, if the (12,8) active space is still used, the MR-CI wave function should be truncated to include higher-order excitations than doubles, which is not available up to now. A particularly useful ansatz is to introduce into the active orbital space a set of diffuse secondary 3d′ orbitals formed by a linear combination of Ni 3d and 4d.[22] For NiH_2, it yields a large active space (12,13) which renders the subsequent MR-CI treatment of dynamical correlation effects computationally too demanding. Luckily, there are several multireference second-order perturbation theory (MR-PT2) methods[25] developed which can utilize this large active space perfectly.

In this paper, we use MCQDPT2,[20] a multi-state MR-PT2 method, to study the low-lying electronic states of possible linear and bent NiH_2 structures.

II. Computational Details

As explained above, 13 orbitals (corresponding to Ni 3d4s3d′ + H 1s + H 1s) with 12 electrons are used as the active space, whereas the inner 4 orbitals (i.e., Ni 3s3p) are always doubly occupied and the electrons therein are correlated.

This is a two-step computation. For linear NiH_2, the SA-CASSCF(12,13) calculations are performed first to guarantee the required degeneracy of the relevant states. This is accomplished by using the C_{2h} point group instead of D_{2h} due to the restriction of the PC-GAMESS program[21] that only states with the same spin multiplicity and same symmetry can be handled simultaneously. Likewise, C_s symmetry with the σ_h plane in the x-direction is used for bent NiH_2 in order to ensure the quasi-degeneracy under C_{2v} symmetry. The map relation of $D_{\infty h}$, D_{2h}, C_{2h}, C_{2v}, and C_s[26] is shown in Table 1. With the help of the relation, we can determine the full symmetry of each electronic state. The MCQDPT2 computations with semidirect integral transformation are then performed by diagonalizing over a basis of several MR-PT2 roots, which ensures that the avoided crossings of states with the same symmetry are treated correctly. In addition, to avoid the effect of intruder states, a suggested energy denominator shift of 0.02[27] is used.

Both the scalar relativistic effects and spin−orbit coupling (SOC) are important for nickel systems.[28] So in the second step, SOC[29] is treated via the state-interaction approach at the SA-CASSCF(12,8) theory level by MOLPRO[18] with the D_{2h} or C_{2v} point group for linear or bent NiH_2, where the CASSCF diagonal matrix elements are replaced by the MCQDPT2 energies.

Since PC-GAMESS has no all-electron scalar relativistic methods such as the popular Douglas−Kroll−Hess (DKH)[30,31] or zero-order regular approximated (ZORA),[32] the relativistic effective core potential (RECP) of Dolg et al.[33] is used for Ni to replace the inner 10 core electrons. The exponents of the valence basis are taken from all-electronic cc-pwCVQZ-DK[34] by deleting the first seven s-, four p- (which correspond to the 1s2s2p core orbitals and their densities on the higher orbitals are less than 10^{-8}), and all h-functions (because PC-GAMESS does not support h basis functions), and are recontracted at the ic-MR-CISD level of theory by using MOLPRO,[18] leading to (17s16p13d4f3g)/[8s8p7d4f3g]. This RECP basis set is used in the scalar computation, whereas in the SOC computation the original all-electronic cc-pwCVQZ-DK basis set is used. For H, the cc-pVQZ and cc-pVQZ-DK[35] basis sets are, respectively, used in the scalar and SOC computations.

In the computation of possibly linear NiH_2, the potential energy curves (PECs) of Λ-S or Ω states are obtained by connecting the calculated energy points for a series of selected bond distances between the nickel and hydrogen atoms with the aid of the avoided-crossing rule between electronic states of the same irreducible representation in the single or double $D_{\infty h}$ point group. From the PECs, the adiabatic excitation energy (T_e) and the bond length (R_e) can be obtained by cubic spline interpretation.

For bent NiH_2, the bond length R_{Ni-H} is first fixed at the linear minimum of the $(I)^3\Delta_g$ state, and only the angle θ_{H-Ni-H} is changed from 60° to 180°. The computation of the equilibrium geometry structure of the candidate ground states in the bent configuration is not as simple as in the linear one. In particular, both the analytic and the numerical gradients for MCQDPT2 are not supported by the present version of PC-GAMESS,[21] so the geometry optimization process is driven by hand: R_{Ni-H} and θ_{H-Ni-H} are optimized alternately until the energy difference, step change, and gradient are less than 5×10^{-7}, 3×10^{-4}, and 4×10^{-4} a.u., respectively.

At the minima of both linear and bent NiH_2, the MCQDPT2 vibrational frequencies can be obtained by finite difference method with the displacement of 0.02 Bohr. This procedure is still driven by hand, and the point group symmetry is not used.

III. Results and Discussion

Since we have determined as shown later that the ground state of NiH_2 is bent, the results of calculations on the linear form are given in the supplemental Supporting Information II. These include the PECs of 14 gerade and 6 ungerade low-lying Λ-S states as well as 26 gerade and 12 ungerade low-lying Ω states of linear NiH_2, the corresponding spectroscopic constants, the dominant configurations, and the Mulliken atomic orbital population analysis.

The lowest state obtained for linear NiH_2 is $(I)^3\Delta_g$, which is in line with the early theoretical results.[11,12] Its equilibrium bond length is 1.540 Å, significantly larger than the theoretical value of about 1.51 Å[12] previously computed by the scalar relativistic CASPT2(12,11) method. After the SOC is taken into account, the lowest Ω state of linear structure is $(I)3_g$, which is basically a pure 3_g component of $(I)^3\Delta_g$.

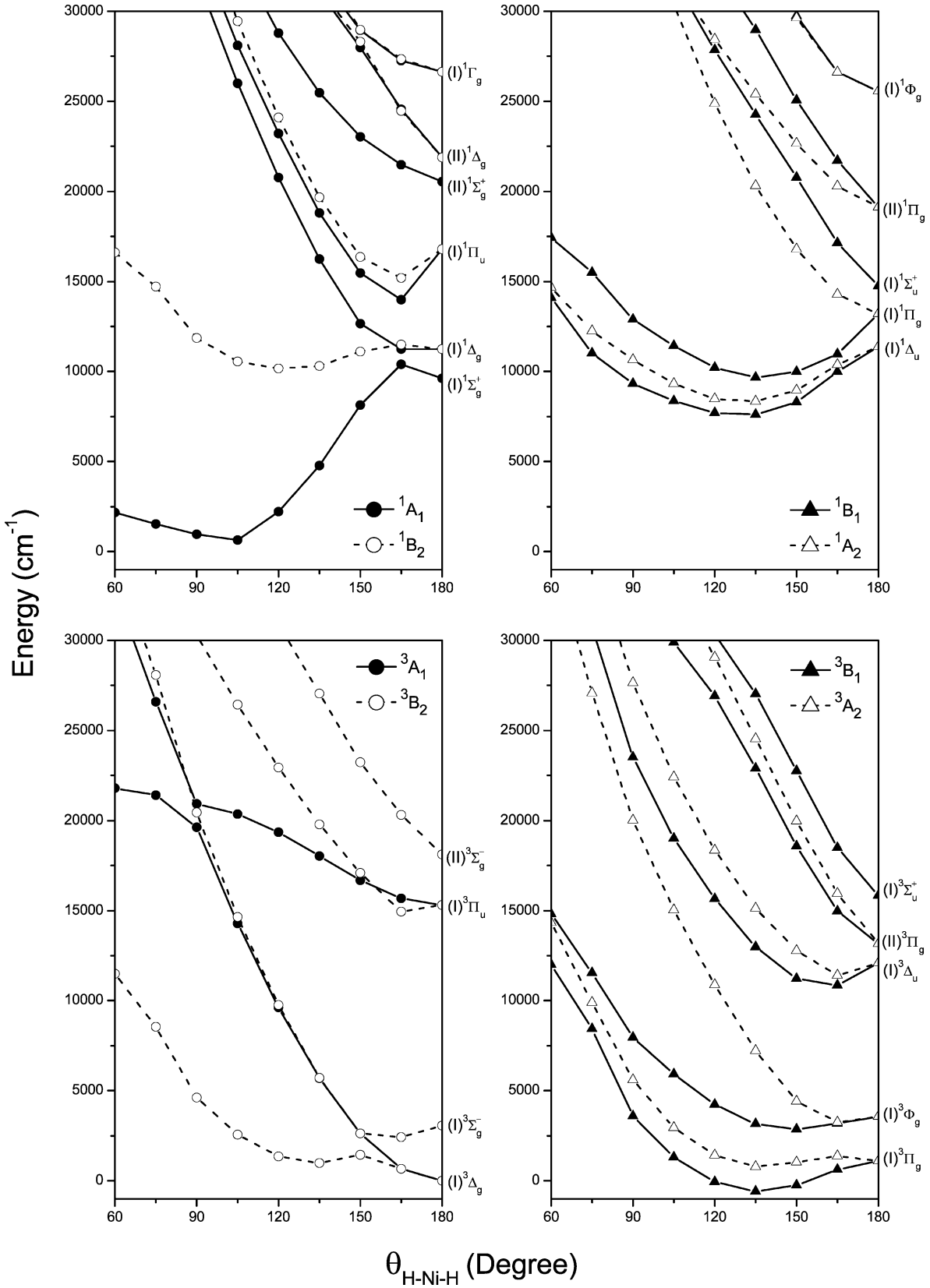

Figure 1. Energy variations of bent NiH_2 with the bending angle θ_{H-Ni-H}. The bond length R_{Ni-H} is fixed at 1.540 Å and SOC is neglected.

Using MCQDPT2(12,13) with a fixed Ni−H bond length of 1.540 Å and temporarily ignoring the SOC, the angle θ_{H-Ni-H} was changed from 60° to 180°. The variations of the energy are shown in Figure 1. It can be seen that both the $(I)^1A_1$ and $(I)^3B_1$ states may be the ground state, although the latter is a bit lower. Then both of their geometries were completely optimized at the MCQDPT2(12,13) level of theory and the results are given in Table 2. Results of other less accurate methods, which will be described later, are also given in this table. It is found that the $(I)^1A_1$ state lies below the $(I)^3\Delta_g$ state by about 2192 cm^{-1}, whereas the $(I)^3B_1$ state is 1568 cm^{-1} higher than $(I)^1A_1$. So, still ignoring SOC, NiH_2 has a bent ground state $(I)^1A_1$ which is more stable than the linear state $(I)^3\Delta_g$. This is in line with the result of Barysz and Papadopou-

TABLE 2: Energies and Structures of Some Low-Lying Λ-S States of NiH_2

state	method	T_e (cm^{-1})	R_{Ni-H} (Å)	θ_{H-Ni-H} (degree)
$(I)^1A_1$	MCQDPT2(12,13)	−2192	1.397	79.3
	ic-MR-AQCC(12,8)	718	1.421	84.7
	HF	26406	1.554	119.4
	VWN5	−10941	1.399	76.7
	BLYP	−5084	1.428	87.6
	B3LYP3 & B3LYP5	1127, 1170	1.423	90.2
	CCSD	2926	1.434	86.4
	CCSD(T)	−625	1.430	83.9
	CASPT2(12,11)[a]	−1889	1.404	72.8
$(I)^3B_1$	MCQDPT2(12,13)	−624	1.522	135.3
$(I)^3\Delta_g$	MCQDPT2(12,13)	0	1.540	180.0
	ic-MR-AQCC(12,8)	0	1.552	180.0
	HF	0	1.614	180.0
	VWN5	0	1.533	180.0
	BLYP	0	1.557	180.0
	B3LYP3 & B3LYP5	0	1.559	180.0
	CCSD	0	1.554	180.0
	CCSD(T)	0	1.550	180.0
	CASPT2(12,11)[a]	0	1.51	180.0

[a] Ref 12.

los[12] in which the reported energy difference between $(I)^1A_1$ and $(I)^3\Delta_g$ is 1889 cm^{-1}. At the equilibrium structures of MCQDPT2(12,13), CASSCF(12,13) gives a linear configuration which is about 3200 cm^{-1} lower than the bent ones. This result is very similar to the one reported by Li et al.[3] In that paper, the CASSCF(12,12) method (written as CASSCF(6×6) in ref 3, i.e., six occupied and six virtual orbitals) was used. Both of the CASSCF results demonstrate that the absent dynamical correlation energy cannot be neglected.

The equilibrium bond length and bond angle of $(I)^1A_1$ are 1.397 Å and 79.3°, respectively, being close to the values of 1.404 Å and 72.8° reported by Barysz and Papadopoulos,[12] whereas the $(I)^3B_1$ state has a longer bond length (1.522 Å) and larger bond angle (135.3°). Li et al.[3] reported experimental bond angles of 92° for NiH_2 and 87° for NiD_2. However, both the angles are not accurate since they were estimated from the intensities. Mulliken population analysis shows that the atomic-like nickel 3*d* orbitals are occupied by 8.76 electrons in the $(I)^1A_1$ state, which means that this state is related to the linear states with ungerade symmetry (cf. Table 2 in Supporting Information II). From the map relation between $D_{\infty h}$ and C_{2v} in Table 1, we can conclude that the bent ground state $(I)^1A_1$ comes from the symmetry-broken $(I)^1\Pi_u$ state. So the essence of the ground-state problem of NiH_2 is how to compute the different correlation energies in nickel $3d^9$ and $3d^8$ super-configurations accurately. Obviously, the $^1A_1$ branch of $(I)^1\Pi_u$ has two avoided crossings at about $\theta_{H-Ni-H} = 165°$ with the $^1A_1$ branches of $(I)^1\Sigma^+_g$ and $(I)^1\Delta_g$ states and many conical intersections which can be estimated from Figure 1.

According to the theory of vibronic interactions, the distortion of the linear NiH_2 molecule is a result of either Renner−Teller (RT) or pseudo Jahn−Teller (PJT) effects.[36] It is found from Figure 1 that the $(I)^3B_2$ state comes from $(I)^3\Sigma^-_g$ instead of $(I)^3\Delta_g$ and has an avoided crossing at about $\theta_{H-Ni-H} = 160°$ with the $^3B_2$ branch of $(I)^3\Delta_g$. Since both the $^3A_1$ and $^3B_2$ branches of $(I)^3\Delta_g$ are stable at the point $\theta_{H-Ni-H} = 180°$, which corresponds to the linear structure, the origin of distortion of linear NiH_2 can only be the PJT effect.

Because of SOC, the $(I)^1A_1$ state becomes A_1, and the $(I)^3B_1$ state splits into three components (A_1, B_2, and A_2). Their MCQDPT2(12,13)-SOC energies (computed at the corresponding equilibrium structures of the Λ-S state) relative to the linear $(I)3_g$ state are listed in Table 3. Now the ground spinor state is $(I)A_1$, being 1509 cm^{-1} lower than the $(I)3_g$ state. Since $(I)A_1$ is characterized mainly by $(I)^1A_1$ (99%), its equilibrium bond length and bond angle are estimated to remain unchanged.

TABLE 3: Energies and Components of Some Low-Lying Spinor Electronic States of NiH_2 Computed at the Corresponding Equilibrium Structures of the Λ-S State

	state	T_e (cm^{-1})	components[a] (%)
bent	$(I)A_1$	−1509	$(I)^1A_1$ (99)
	$(II)A_1$	−235	$(I)^3B_1$ (86) + $(I)^3B_2$ (11) + $(I)^3A_2$ (3)
	$(I)A_2$	−220	$(I)^3B_1$ (86) + $(I)^3B_2$ (13)
	$(I)B_2$	−77	$(I)^3B_1$ (90) + $(I)^3A_2$ (9)
linear	$(I)3_g$	0	$(I)^3\Delta_g$ (98) + $(I)^3\Phi_g$ (2)

[a] Weights lower than 2% are not listed.

There are not sufficiently accurate experimental results up to now so that the accuracies of the computed energies and structures can be known. However, a rough estimate may be obtained from the theoretical research of the diatomic molecule NiH[37] where the low-lying electronic states were studied using the all-electron scalar relativistic multi-state CASPT2(11,12) method with SOC. Compared with the available experimental values, the MAEs of T_e and R_e of the diatomic NiH molecule were about 800 cm^{-1} and 0.03 Å, respectively.[37] As for linear NiH_2, the MAEs of the present T_e and R_e differ by 312 cm^{-1} and 0.004 Å, respectively, compared with our early unpublished results where the all-electron scalar relativistic basis sets are the same as the ones in ref 37. In summation, it is expected that our results of NiH_2 should have an accuracy similar to that in the case of NiH,[37] that is, about 800 cm^{-1} and 0.03 Å.

Both the bent $(I)^1A_1$ and the linear $(I)^3\Delta_g$ states have also been optimized by using some cheaper theoretical methods. The single-configurational methods include Hartree−Fock (HF), DFT with local density approximation (LDA) VWN functional V[38] (donated as VWN5), with generalized gradient approximation (GGA) BLYP,[39,40] and with hybrid functional B3LYP[40,41] (in which VWN functional III and V[38] are used for local correlation, denoted, respectively, as B3LYP3 and B3LYP5), coupled-cluster with single and double excitations (CCSD),[42] and CCSD with perturbative triples corrections, that is, CCSD(T).[43] The single-reference configuration of $(I)^3\Delta_g$ corresponds to nickel $(3d_\delta)^3(3d_\sigma)$,[1] while for $(I)^1A_1$, the lowest five a_1, two b_1 and b_2, and one a_2 molecular orbitals are fully occupied. The multi-configurational method used is internal-contracted multireference average quadratic single and double coupled-cluster (ic-MR-AQCC)[44] with the active space of (12,8). These geometry optimization computations were carried out by using MOLPRO,[18] and the results are also listed in Table 2.

It can be seen that all the methods except the single-reference HF method give fairly good equilibrium structures for the $(I)^1A_1$ and $(I)^3\Delta_g$ states; however, the estimated energy gaps between the two states are very different from each other. HF gives the largest positive gap, whereas VWN5 gives the lowest negative gap. BLYP reduces the gap of VWN5 by half, but the value is still much larger than the one derived from MCQDPT2(12,13). Since an exact exchange (which has the same form as HF) is incorporated into the functional,[41] B3LYP reduces the gap of BLYP further. However, this correction is overestimated so much that $(I)^3\Delta_g$ becomes the ground state. CCSD improves the gap of HF considerably, but still cannot capture the right ground state. As the most accurate single-configurational method used in this work, CCSD(T) gives the bent structure with an energy gap of −625 cm^{-1}. However, if SOC is taken into account, the gap will be changed to about 60 cm^{-1} so the linear

TABLE 4: Theoretical Vibrational Frequencies of the (I)$^1A_1$ State Compared with Experimental Values

		MCQ DPT2 (12,1 3)		ic-M R-A QCC (12,8)		CCS D		CCS D(T)		B3L YP5		
	frequency (cm^{-1})	harm.	VSC F	har m.	VSC F	har m.	VSCF	har m.	VSCF	har m.	VSCF	expt.[c]
NiH_2	ν_1 (sym. str.)[a]	2224	215 9	2097	2032	2102	2037	1941	1876	2102	2037	2007
	ν_2 (bend)[a]	913	876	391	354	727	690	665	628	776	739	771
	ν_3 (asym. str.)[b]	2373	227 2	2086	1985	2100	1999	2058	1957	2091	1990	1969
NiH D	ν_1 (sym. str.)[a]	2302	218 4	2091	1973	2101	1983	2003	1885	2104	1986	1988
	ν_2 (bend)[a]	782	722	339	279	630	570	577	517	677	617	624
	ν_3 (asym. str.)[b]	1640	159 1	1492	1443	1499	1450	1423	1374	1502	1453	1435
NiD_2	ν_1 (sym. str.)[a]	1595	156 3	1498	1466	1501	1469	1386	1354	1506	1474	1445
	ν_2 (bend)[a]	646	636	278	268	517	507	473	463	555	545	602
	ν_3 (asym. str.)[b]	1690	163 8	1486	1434	1497	1445	1466	1414	1496	1444	1426
MA E	ν_1 (sym. str.)	227	155	82	20	88	20	46	108	91	20	
	ν_2 (bend)	115	79	330	365	45	77	94	130	35	32	
	ν_3 (asym. str.)	291	224	78	11	89	21	47	28	86	19	

[a] For NiH_2/NiD_2 and NiHD, the vibrational modes are, respectively, a_1 and a′. [b] For NiH_2/NiD_2 and NiHD, the vibrational modes are, respectively, b_2 and a′. [c] Ref 3.

state (I)3_g will be the ground state. It means in the single-configuration picture, the coupled-cluster method with higher-order excitations should be used in order to predict the right ground state of NiH_2. The multi-configurational method ic-MR-AQCC(12,8) also predicts a linear structure. It is found that the relative energy difference of (I)$^1A_1$ between ic-MR-AQCC-(12,8) and MCQDPT2(12,13) is about 2900 cm^{-1}, being close to the MAE difference of about 3000 cm^{-1} between gerade and ungerade states of ic-MR-CISD+Q(12,8) (cf. Table 1 in Supporting Information I). As explained above, these theoretical departures should be attributed to the lack of consideration of the strong correlation from nickel $3d^9$. In the cases of both CCSD and ic-MR-AQCC(12,8), for instance, there are two electrons excited into the nickel 3d′ (or 4d) orbitals at most, so the correlation treatment is not sufficient. Obviously the higher-order excitations to nickel 3d′ orbitals are not negligible.

It is noted that a bent ground state (I)$^1A_1$ was obtained by using B3LYP3 and QCISD in ref 11. In fact, as pointed out by Barysz and Papadopoulos,[12] the results in ref 11 strongly depend on the basis sets and the Hamiltonians. Since we have used much larger basis sets and taken the scalar relativistic effects into account, our B3LYP3 and CCSD results should be more accurate than the early ones of B3LYP3 and QCISD. The theoretical computations in ref 11 captured the right ground state of NiH_2 just because of their small basis sets and the lack of the scalar relativistic effects. With better basis sets and scalar relativistic effects, the methods erroneously give a linear structure.

At the corresponding equilibrium structure of each theoretical method, that is, MCQDPT2(12,13), ic-MR-AQCC(12,8), CCSD, CCSD(T), and B3LYP5, the vibrational frequencies are computed. The theoretical and experimental frequencies of NiH_2, NiHD, and NiD_2 are summarized in Table 4. The anharmonic effects are so strong, as mentioned in ref 3, that our harmonic frequencies cannot be directly compared with the experimental values. In order to approximate anharmonic effects, a vibrational self-consistent field (VSCF)[45] computation was carried out at the B3LYP5 level of theory. For each vibrational mode, the anharmonicity correction has little to do with the selected Hamiltonians as well as the basis sets, and it is almost a constant within the accuracy we desire (for example, refer to Table 5 in ref 46). Thus we can apply this anharmonicity correction derived from B3LYP5 to the other harmonic frequencies.

After introducing the anharmonic effects, the frequencies of B3LYP5 are in excellent agreement with the experimental values, with the MAEs of symmetric stretching (ν_1), bending (ν_2), and asymmetric stretching (ν_3) modes of only 20, 32, and 19 cm^{-1}, respectively. It must be admitted, however, that this agreement may be an artifact of the approximate method used to treat the severe anharmonicity of this system. CCSD also obtains good frequencies. However, the frequencies of CCSD-(T) become a little worse than the ones of CCSD. Since all the frequencies of CCSD(T) are less than the corresponding ones of CCSD, we believe this departure may be a result of the non-variational triples in CCSD(T) which makes the PES flatter than that of CCSD (for example, see the case of the multi-configurational C_2 molecule in ref 47). ic-MR-AQCC(12,8) gives a bit better symmetric and asymmetric stretching frequencies, but the bending frequencies are very bad. The ν_2 frequencies of MCQDPT2(12,13) are fairly good, whereas the ν_1 and ν_3 frequencies are, respectively, about 115 and 224 cm^{-1} larger in average. This is a surprising result because the present MCQDPT2(12,13) calculations, using a large active space, should be more accurate than all the other methods.

An interesting thing is that, for NiH_2 and NiD_2, both MCQDPT2(12,13) and CCSD(T) predict a larger ν_3 (harmonic and anharmonic) frequency than ν_1. The experimental assignment[3] was simply derived from a CASSCF(12,12) computation instead of experimental analysis. In their theoretical computation, the very important dynamical correlation energy was not taken into account, and we cannot judge whether the 12 active orbitals include the nickel 3d′ (or 4d) ones, so the arrangement of the frequencies remains to be clarified by future more accurate experimental and theoretical research.

Conclusions

The complicated electronic structure of systems containing 3d-metal atoms is a challenge for modern quantum chemistry techniques, because the distinct $3d^n$ and $3d^{n+1}$ super-configurations cannot easily be described in balance by using regular theoretical methods. In this paper, the PECs and spectroscopic constants of the low-lying electronic states of NiH_2 are calculated within the MCQDPT2 framework with a large active space of CAS(12,13), taking the strong correlation into account, and including the relativistic effects. At this level of theory, we find the $^1A_1$ state with bent structure is more stable than the linear $^3\Delta_g$ state, which is in line with the experimental measurement. The computed structure and vibrational frequencies are compared with experimental and other theoretical methods. Our results indicate, in the theoretical frameworks of CC or MR-CI with small active space, higher-order excitations than perturbative triples would have to be included in the wave function in order to take the strong correlation into account.

Our frequency results predict that the experimental stretching frequencies of NiH_2 and NiD_2 should be reanalyzed with a more accurate investigation of the vibrational anharmonicity.

Acknowledgment. This research has been supported by Grant F-100 from the Welch Foundation. We thank John Stanton for his suggestions and permission to use his version of the ACES II-MAB program.

Supporting Information Available: Results of NiH_2 with linear configuration are provided, including the PECs, energies, and bond lengths. This material is available free of charge via the Internet at http://pubs.acs.org.

References and Notes

(1) Schlenk, W.; Weichselfelder, T. *Ber. Dtsch. Chem. Ges.* **1923**, *56*, 2230.
(2) Weichselfelder, T. *Ber. Dtsch. Chem. Ges.* **1929**, *62*, 769.
(3) Li, S.; Van Zee, R. J.; Weltner, W., Jr.; Cory, M. G.; Zerner, M. C. *J. Chem. Phys.* **1997**, *106*, 2055.
(4) Guse, M. P.; Blint, R. J.; Kunz, A. B. *Int. J. Quantum Chem.* **1977**, *11*, 725.
(5) Blomberg, M. R. A.; Brandemark, U.; Pettersson, L.; Siegbahn, P. E. M. *Int. J. Quantum Chem.* **1983**, *23*, 855.
(6) Blomberg, M. R. A.; Siegbahn, P. E. M. *J. Chem. Phys.* **1983**, *78*, 986.
(7) Blomberg, M. R. A.; Siegbahn, P. E. M. *J. Chem. Phys.* **1983**, *78*, 5682.
(8) Ruette, F.; Blyholder, G.; Head, J. *J. Chem. Phys.* **1984**, *80*, 2042.
(9) Filatov, M. J.; Zilberberg, I. L.; Zhidomirov, G. M. *Int. J. Quantum Chem.* **1992**, *44*, 565.
(10) Niu, J.; Rao, B. K.; Jena, P.; Manninen, M. *Phys. Rev. B* **1995**, *51*, 4475.
(11) Barron, J. R.; Kelley, A. R.; Liu, R. *J. Chem. Phys.* **1998**, *108*, 1.
(12) Barysz, M.; Papadopoulos, M. G. *J. Chem. Phys.* **1998**, *109*, 3699.
(13) Ran, M.; Huan, G. P.; Zhu, Z. H. *Chin. J. Atom. Mol. Phys.* **2003**, *20*, 81 (in Chinese).
(14) Zheng, G.; Witek, H. A.; Bobadova-Parvanova, P.; Irle, S.; Musaev, D. G.; Prabhakar, R.; Morokuma, K.; Lundberg, M.; Elstner, M.; Köhler, C.; Frauenheim, T. *J. Chem. Theory Comput.* **2007**, *3*, 1349.
(15) Werner, H.-J.; Knowles, P. J. *J. Chem. Phys.* **1985**, *82*, 5053.
(16) Knowles, P. J.; Werner, H.-J. *Chem. Phys. Lett.* **1985**, *115*, 259.
(17) Knowles, P. J.; Werner, H.-J. *Theor. Chim. Acta* **1992**, *84*, 95.
(18) Werner, H.-J.; Knowles, P. J.; Lindh, R.; Manby, F. R.; Schütz, M.; Celani, P.; Korona, T.; Rauhut, G.; Amos, R. D.; Bernhardsson, A.; Berning, A.; Cooper, D. L.; Deegan, M. J. O.; Dobbyn, A. J.; Eckert, F.; Hampel, C.; Hetzer, G.; Lloyd, A. W.; McNicholas, S. J.; Meyer, W.; Mura, M. E.; Nicklass, A.; Palmieri, P.; Pitzer, R.; Schumann, U.; Stoll, H.; Stone, A. J.; Tarroni, R.; Thorsteinsson, T. MOLPRO, version 2006.1; a package of ab initio programs; see http://www.molpro.net.
(19) Brooks, B. R.; Schaefer, H. F. *J. Chem. Phys.* **1979**, *70*, 5092.
(20) Nakano, H. J. *Chem. Phys.* **1993**, *99*, 7983.
(21) Granovsky, A. A. PC-GAMESS, version 7.0; see http:// classic-.chem.msu.su/gran/gamess/index.html.
(22) Fischer, C. F. *J. Phys. B* **1977**, *10*, 1241.
(23) Andersson, K.; Roos, B. O. *Chem. Phys. Lett.* **1992**, *191*, 507.
(24) Blomberg, M.; Siegbahn, P.; Roos, B. *Mol. Phys.* **1982**, *47*, 127.
(25) Davidson, E. R.; Jarzecki, A. A. Recent Advances in Multi-reference Methods. In *Recent Advances in Computational Chemistry*, Vol. 4; Hirao, K., Ed.; World Scientific Publishing: Singapore, 1999.
(26) Altmann, S. L.; Herzig, P. *Point Group Theory Tables*; Clarendon Press: Oxford, 1994.
(27) Witek, H. A.; Choe, Y.-K.; Finley, J. P.; Hirao, K. J. *Comput. Chem.* **2002**, *23*, 957.
(28) Martin, R. L.; Hay, P. J. *J. Chem. Phys.* **1981**, *75*, 4539.
(29) Berning, A.; Schweizer, M.; Werner, H.-J.; Knowles, P. J.; Palmieri, P. *Mol. Phys.* **2000**, *98*, 1823.
(30) Douglas, M.; Kroll, N. M. *Ann. Phys.* **1974**, *82*, 89.
(31) Hess, B. A. *Phys. Rev. A* **1986**, *33*, 3742.
(32) van Lenthe, E.; Baerends, E. J.; Snijders, J. G. *J. Chem. Phys.* **1994**, *101*, 9783.
(33) Dolg, M.; Wedig, U.; Stoll, H.; Preuss, H. J. *Chem. Phys.* **1987**, *86*, 866.
(34) Balabanov, N. B.; Peterson, K. A. *J. Chem. Phys.* **2005**, *123*, 064107.
(35) Dunning, T. H.; Jr. *J. Chem. Phys.* **1989**, *90*, 1007.
(36) Bersuker, I. B. *The Jahn-Teller Effect*; Cambridge University Press: New York, 2006.
(37) Zou, W.; Liu, W. *J. Comput. Chem.* **2007**, *28*, 2286.
(38) Vosko, S. H.; Wilk, L.; Nusair, M. *Can. Phys. J.* **1980**, *58*, 1200.
(39) Becke, A. D. *Phys. Rev. A* **1988**, *38*, 3098.
(40) Lee, C.; Yang, W.; Parr, R. G. *Phys. Rev. B* **1988**, *37*, 785.
(41) Becke, A. D. *J. Chem. Phys.* **1993**, *98*, 5648.
(42) Knowles, P. J.; Hampel, C.; Werner, H.-J. *J. Chem. Phys.* **1993**, *99*, 5219.
(43) Deegan, M. J. O.; Knowles, P. J. *Chem. Phys. Lett.* **1994**, *227*, 321.
(44) Werner, H.-J.; Knowles, P. J. *Theor. Chim. Acta* **1990**, *78*, 175.
(45) Chaban, G. M.; Jung, J. O.; Gerber, R. B. *J. Chem. Phys.* **1999**, *111*, 1823.
(46) Chaban, G. M.; Xantheas, S. S.; Gerber, R. B. *J. Phys. Chem. A* **2003**, *107*, 4952.
(47) Abrams, M. L.; Sherrill, C. D. *J. Chem. Phys.* **2004**, *121*, 9211.